DØ Note 5134-CONF

Search for Scalar Top Pair Production in the Acoplanar Jet Topology with the D0 Detector

The DØ Collaboration
URL: http://www-d0.fnal.gov
(Dated: June 7, 2006)

A search for the pair production of scalar top quarks, $\tilde{t}$, has been performed in 310 pb^{-1} of data from $p\bar{p}$ collisions at a center-of-mass energy of 1.96 TeV, collected by the D0 detector at the Fermilab Tevatron collider. The $\tilde{t}$ decay mode considered is $\tilde{t} \to c\tilde{\chi}_1^0$, where $\tilde{\chi}_1^0$ is the lightest supersymmetric particle. The topology analyzed therefore consists of a pair of acoplanar heavy-flavor jets with missing E_T. The data show good agreement with the standard model expectation, and a 95% C.L. exclusion domain in the $(m_{\tilde{t}}, m_{\tilde{\chi}_1^0})$ plane has been determined, which extends the domain excluded by previous experiments.

Preliminary Results for Summer 2006 Conferences

I. INTRODUCTION

Supersymmetric (SUSY) models [1] predict the existence of new particles, carrying the same quantum numbers as their standard model (SM) partners, but differing by half a unit of spin. For instance, there are two scalar-quark fields associated with the left- and right-handed degrees of freedom of each ordinary quark. The mass eigenstates result from the diagonalization of a mass matrix, with elements determined by the specific SUSY-breaking pattern. A light SUSY partner of the top quark, or stop, is a generic prediction of models inspired from supergravity (SUGRA) [2]. A first reason is that, due to the impact of the large top Yukawa coupling in the renormalization group equations, the diagonal elements of the mass matrix are driven at the electroweak scale to a value smaller than for the other scalar quarks [3]. A second reason is that the off-diagonal terms are proportional to the relevant quark mass, and are hence much larger in the case of the top quark. The mass eigenstates are therefore broadly split, with the mass of the lighter stop $\tilde{t}$ thus driven to an even lower value [4]. Finally, it can be noticed that a light stop is a necessary ingredient in the context of electroweak baryogenesis [5].

In models with R-parity conservation [6], the lightest SUSY particle (LSP) is stable, and cosmological constraints imply that it should be neutral and colorless [7]. In SUGRA inspired models, the lightest of the neutralinos — the mass eigenstates resulting from the mixing of the SUSY partners of the neutral gauge and Higgs bosons — arises as the natural LSP, and furthermore appears as a viable dark matter source. In the following, it will be assumed that R-parity is conserved, and that the LSP is the lightest neutralino $\tilde{\chi}_1^0$.

The dominant stop decay modes are expected to be $\tilde{t} \to t\tilde{\chi}_1^0$ and $\tilde{t} \to b\tilde{\chi}_1^+$, where the chargino $\tilde{\chi}_1^+$ is the lighter of the mass eigenstates resulting from the mixing of the SUSY partners of the charged gauge and Higgs bosons. In the $\tilde{t}$ mass range of interest in this note, the $\tilde{t} \to t\tilde{\chi}_1^0$ decay mode is however kinematically closed. In the following, the region of SUSY parameter space considered is such that $m_{\tilde{t}} < m_b + m_{\tilde{\chi}_1^+}$ and $m_{\tilde{t}} < M_W + m_b + m_{\tilde{\chi}_1^0}$, under which conditions the dominant decay mode becomes $\tilde{t} \to c\tilde{\chi}_1^0$, a flavor-changing loop decay [8]. Tree-level four-body decays $\tilde{t} \to bf\bar{f}'\tilde{\chi}_1^0$ are also possible in principle [9], but they are disfavored for most parameter choices in SUGRA-inspired models.

In $p\bar{p}$ collisions, stop pair production proceeds via $q\bar{q}$ annihilation and gluon-gluon fusion. The cross section has very little dependence on SUSY parameters other than the stop mass. At the center-of-mass energy of 1.96 TeV available in Run II of the Fermilab Tevatron collider, it ranges from 15 to 2.25 pb for stop masses from 100 to 140 GeV, as calculated at next-to-leading order (NLO) with PROSPINO [10], for a renormalization and factorization scale $\mu_{rf} = m_{\tilde{t}}$ and using the CTEQ6.1M parton density functions (PDF's) [11]. The final state topology resulting from the $\tilde{t} \to c\tilde{\chi}_1^0$ decay is a pair of acoplanar jets, with large missing transverse energy $\not\!\!E_T$ carried away by the two weakly interacting LSP's. Previous searches in this topology performed at LEP have excluded stop masses smaller than ~ 100 GeV, essentially independent of the stop-$\tilde{\chi}_1^0$ mass difference [12]. Searches during the Run I of the Tevatron [13, 14] extended the domain excluded at LEP to larger stop masses, but for mass differences not exceeding ~ 50 GeV. The largest stop mass excluded was 122 GeV, for $m_{\tilde{\chi}_1^0} = 45$ GeV [14]. In this note, we report on a similar search, performed in data collected by the D0 detector during Run II of the Tevatron.

The acoplanar jet topology may arise from other new physics processes than stop pair production. Recently, the D0 Collaboration performed a search for pair production of leptoquarks decaying into a quark and a neutrino [15], which leads to the same topology. The analysis reported here is largely based on that leptoquark search. In the following, only a brief summary of the common aspects is therefore given, while the specific features relevant for the stop search are presented in greater detail. The main differences arise from the LSP mass, which leads to smaller jet transverse energies and to a reduced $\not\!\!E_T$, compared to the case of leptoquark decays which involve massless neutrinos. Another characteristic feature of stop decays is that charmed jets are produced, while first-generation leptoquarks decay to light-flavored jets.

II. DATA AND SIMULATED SAMPLES

A thorough description of the D0 detector can be found in Ref. [16]. The central tracking system consists of a silicon microstrip tracker and a fiber tracker, both located within a 2 T superconducting solenoidal magnet. A liquid-argon and uranium calorimeter covers pseudorapidities up to $|\eta| \sim 4.2$, where $\eta = -\ln[\tan(\theta/2)]$ and θ is the polar angle with respect to the proton beam direction. An outer muon system, covering $|\eta| < 2$, consists of layers of tracking detectors and scintillation counters on both sides of 1.8 T iron toroids.

For this search, ~ 14 million events collected with a Jets $+\not\!\!E_T$ trigger have been analyzed, corresponding to an integrated luminosity of $310\,\text{pb}^{-1}$. The offline analysis utilized jets reconstructed with the Run II cone algorithm [17], with a radius of 0.5 in η-ϕ space, where ϕ is the azimuthal angle in radians. Only jets with transverse momentum $p_T > 15$ GeV were considered in the analysis. The missing transverse energy $\not\!\!E_T$ was calculated from all calorimeter

cells, corrected for the energy scale of reconstructed jets, as determined from the transverse momentum balance in photon+jet events, and for the momentum of reconstructed muons.

Signal efficiencies and SM backgrounds have been evaluated using events processed through the detailed detector simulation and reconstructed using the standard event reconstruction. A Poisson average of 0.8 minimum-bias events were superimposed. The instrumental background from multijet production has not been simulated, and was estimated directly from the data. The SM processes expected to yield the largest background contributions are vector boson production in association with jets. They were generated with ALPGEN 1.3 [18], interfaced with PYTHIA 6.202 [19] for the simulation of initial and final state radiation and for jet hadronization. The PDF's used were CTEQ5L [20]. The NLO cross sections for vector boson production in association with jets were calculated with MCFM 3.4.4 [21]. Vector-boson pair, $t\bar{t}$, and single-top productions have also been considered. Signal samples of 10,000 events were generated with PYTHIA for stop masses ranging from 95 to 145 GeV and for $\tilde{\chi}_1^0$ masses from 40 to 70 GeV, both in steps of 5 GeV.

III. EVENT SELECTION

The following selection criteria were applied, independent of the stop and $\tilde{\chi}_1^0$ masses: there had to be at least two jets; the vector sum of all jet transverse momenta had to exceed 40 GeV, as well as the missing transverse energy; the highest pT (leading) and 2nd highest pT (subleading) jets had to be central ($|\eta_{\rm det}| < 1.5$, where $\eta_{\rm det}$ is the pseudorapidity measured from the detector center), with transverse momenta exceeding 40 and 20 GeV, respectively, and they had to be confirmed by charged particle tracks [15]; the acoplanarity $\Delta\Phi$ of the two leading jets had to be smaller than 165°, where $\Delta\Phi$ is the difference between the two jet azimuthal angles; the longitudinal position of the primary vertex had to be less than 60 cm away from the center of the detector. At this point, 99 884 events were selected, largely dominated by instrumental background from multijet events. The efficiency for a reference signal with $m_{\tilde{t}} = 130$ GeV and $m_{\tilde{\chi}_1^0} = 50$ GeV was 34%. The jet multiplicity distribution revealed that most of the selected events contained at least three jets, due to the acoplanarity requirement. Only events containing exactly two jets were therefore retained, leaving 27 853 data events with an efficiency of 24% for the reference signal. The inefficiency associated with the rejection of events with more than two jets was evaluated, based on studies of jet multiplicities in real and simulated $Z \to ee$+2-jet events, where the jets fulfilled the same selection criteria as in the analysis. Standard model backgrounds from $W \to \ell\nu$+jet processes were greatly reduced by requiring that there be no isolated electron or muon with $p_T > 10$ GeV, and no isolated charged particle track with $p_T > 5$ GeV [15]. This retained 22 106 data events, with an efficiency of 21% for the reference signal. A large fraction of the remaining instrumental background was eliminated by the requirement that $\Delta\Phi_{\rm max} - \Delta\Phi_{\rm min}$ be smaller than 120°, where $\Delta\Phi_{\rm min}$ and $\Delta\Phi_{\rm max}$ are the minimum and maximum of the angles between the $\not\!\!E_T$ direction and the directions of the two jets, respectively: this cut takes advantage of the fact that, in the instrumental background, the $\not\!\!E_T$ direction tends to be close to the direction of a mismeasured jet. The efficiency for the reference signal was 20% at this point, and 9 337 data events were retained.

To increase the search sensitivity, advantage was then taken of the presence of charmed jets in the signal. A lifetime-based heavy-flavor tagging algorithm was used for that purpose, which involves a probability built from the impact parameter significances of the tracks belonging to the jet. The impact parameter of a track is its distance of closest approach to the event vertex, in a plane perpendicular to the beam axis, and the significance is obtained by the normalization to the impact parameter uncertainty. This probability is constructed such that its distribution is uniform for light-flavored jets, and peaks towards zero for heavy-flavored jets. In order to cope with differences in track reconstruction efficiencies in data and in simulation, the heavy-flavor tagging algorithm was applied directly only to the data, while flavor-dependent tagging probabilities measured in dedicated data samples were applied to the simulated jets. The probability cut used in this analysis was such that typically 4% of the light-flavored jets were tagged (central jets with $p_T \sim 50$ GeV). The corresponding typical tagging efficiencies for c and b-quark jets were 30% and 65%, respectively. Jets resulting from τ decays were tagged with a typical efficiency of 20%. By requiring that at least one jet be tagged, 1 154 data events were selected, and the efficiency for the reference signal was 9.1%.

Since the signal topology depends on the stop and $\tilde{\chi}_1^0$ masses, cuts on four variables were simultaneously optimized for each mass combination. These variables were the transverse momenta p_T^1 and p_T^2 of the leading and subleading jets, and the missing E_T, all in steps of 10 GeV, and $\Delta\Phi_{\rm max} + \Delta\Phi_{\rm min}$ in steps of 10°. This last variable had been seen to provide good discrimination between signal and SM backgrounds [15]. The optimal set of cuts was chosen as the one which minimized the signal confidence level CL_s expected if only background were present [22]. The systematic uncertainties discussed further down were taken into account in the optimization procedure. The contribution of the instrumental background was estimated as in Ref. [15] by extrapolation beyond the tested $\not\!\!E_T$ cut value of a parameterization of the $\not\!\!E_T$ distribution determined, after subtraction of the SM background contribution, in the region $\not\!\!E_T < 55$ GeV where the instrumental background is largely dominant. The average of the predictions

TABLE I: Numbers of events from standard model, instrumental and total backgrounds expected; number of data events selected; and number of reference signal events expected ($m_{\tilde{t}} = 130\,\text{GeV}$ and $m_{\tilde{\chi}_1^0} = 50\,\text{GeV}$), for the nominal production cross section. For the total-SM and total backgrounds, as well as for the signal, the first errors are statistical, and the second systematic. The errors on the individual SM backgrounds are statistical. The error on the instrumental background is mostly systematic from the parameterization extrapolation. The selection cuts are those optimized for the reference signal. In the SM backgrounds, "jet" stands for "light-flavored jet". The SM backgrounds not listed are negligible.

$Z \to \nu\nu$+2-jets	15.7 ± 2.8
$Z \to \nu\nu + b\bar{b}$	3.8 ± 0.2
$Z \to \nu\nu + c\bar{c}$	1.8 ± 0.3
$W \to \ell\nu$+jets	24.6 ± 7.8
$W \to \ell\nu + b\bar{b}$	1.9 ± 0.2
$W \to \ell\nu + (c\bar{c}$ or c+jet)	1.6 ± 0.4
$t\bar{t}$ and single top	4.1 ± 0.3
WW, WZ, ZZ	2.5 ± 0.3
Total SM background	$56.1 \pm 8.3 \pm 9.7$
Instrumental background	3.3 ± 1.6
Total background	$59.4 \pm 8.3 \pm 9.8$
Data events selected	60
Reference signal	$39.5 \pm 2.0 \pm 4.8$

from exponential and power-law functional forms was used, and a systematic uncertainty was set to account for the difference. The trigger response was modeled in the simulation according to parameterizations determined from data, using events collected with triggers which do not involve jets or missing E_T. For the reference signal, the selection criteria thus obtained were $p_T^1 > 40\,\text{GeV}$, $p_T^2 > 20\,\text{GeV}$, $\not\!\!E_T > 70\,\text{GeV}$, and $\Delta\Phi_{\max} + \Delta\Phi_{\min} < 280°$, leading to a signal efficiency of 3.7% while retaining 60 data events. For the smallest stop masses considered, the optimization procedure led to a lower value for the $\not\!\!E_T$ cut and to a higher value for the $\Delta\Phi_{\max} + \Delta\Phi_{\min}$ cut. For the highest stop masses, larger values for the p_T^1 and p_T^2 cuts were selected.

Marginal distributions, i.e. distributions obtained after all cuts except for the one on the variable displayed, are shown in Fig. 1 for $\Delta\Phi_{\max} - \Delta\Phi_{\min}$ and $\Delta\Phi_{\max} + \Delta\Phi_{\min}$, and in Fig. 2 (top frame) for the missing E_T. The final $\not\!\!E_T$ distribution is shown in Fig. 2 (bottom frame). All these distributions were obtained for the reference signal with the corresponding selection. An excess at large $\not\!\!E_T$ is observed in the data with respect to the expectation: there are eight data events with $\not\!\!E_T > 150\,\text{GeV}$, while 3.0 ± 1.2 background events are expected. The $\not\!\!E_T$ of these events is also larger than expected from a stop signal. A visual scan did not reveal any anomaly.

IV. RESULTS

A. Backgrounds

The background composition is detailed in Table I for the selection optimized for the reference signal. As expected, the largest contributions come from ($Z \to \nu\nu$ and $W \to \ell\nu$)+light-flavored jets. This is due to the loose heavy-flavor tagging criterion which was selected in order to be efficient for charmed jets. Vector boson production with heavy-flavored jets give rather small contributions because of the comparatively small cross sections. The instrumental background represents only 6% of the total background for the reference signal.

B. Systematic uncertainties

Systematic uncertainties were evaluated for each combination of stop and $\tilde{\chi}_1^0$ masses, according to the corresponding optimized selection criteria. They are listed below for the reference signal. The following ones are fully correlated between SM-background and signal expectations: from the jet energy scale and resolution, $^{+9}_{-5}$% for the SM background and $^{+4}_{-5}$% for the signal; from the jet multiplicity cut, 2% for the SM background and 1% for the signal; from the trigger efficiency, 2% after all selection cuts; from the heavy-flavor tagging, 6% for the SM background and 7% for the signal; from the integrated luminosity of the analysis sample, 6.5%. In addition to the 15% statistical uncertainty of the simulation, the normalization of the SM-background expectation carries a 13% uncertainty. The small instrumental background is affected by an uncertainty of 48%, related to the extrapolation procedure from the low to the high $\not\!\!E_T$

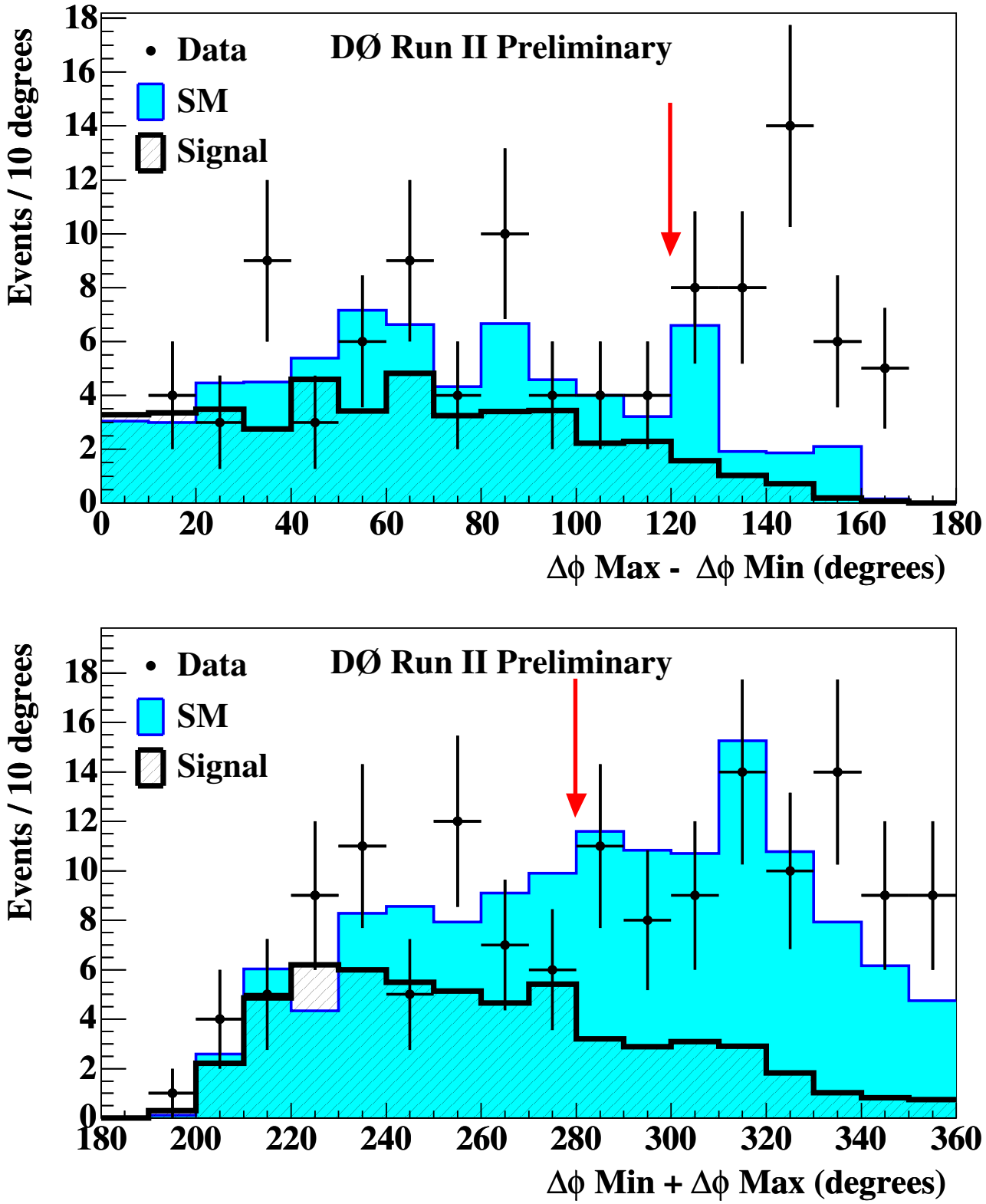

FIG. 1: Marginal distributions of $\Delta\Phi_{\rm max} - \Delta\Phi_{\rm min}$ (top) and of $\Delta\Phi_{\rm max} + \Delta\Phi_{\rm min}$ (bottom) for data (points with error bars), for SM backgrounds (shaded histograms) and for a signal with $m_{\tilde{t}} = 130\,{\rm GeV}$ and $m_{\tilde{\chi}_1^0} = 50\,{\rm GeV}$ (hatched histograms). The cut locations are indicated by arrows.

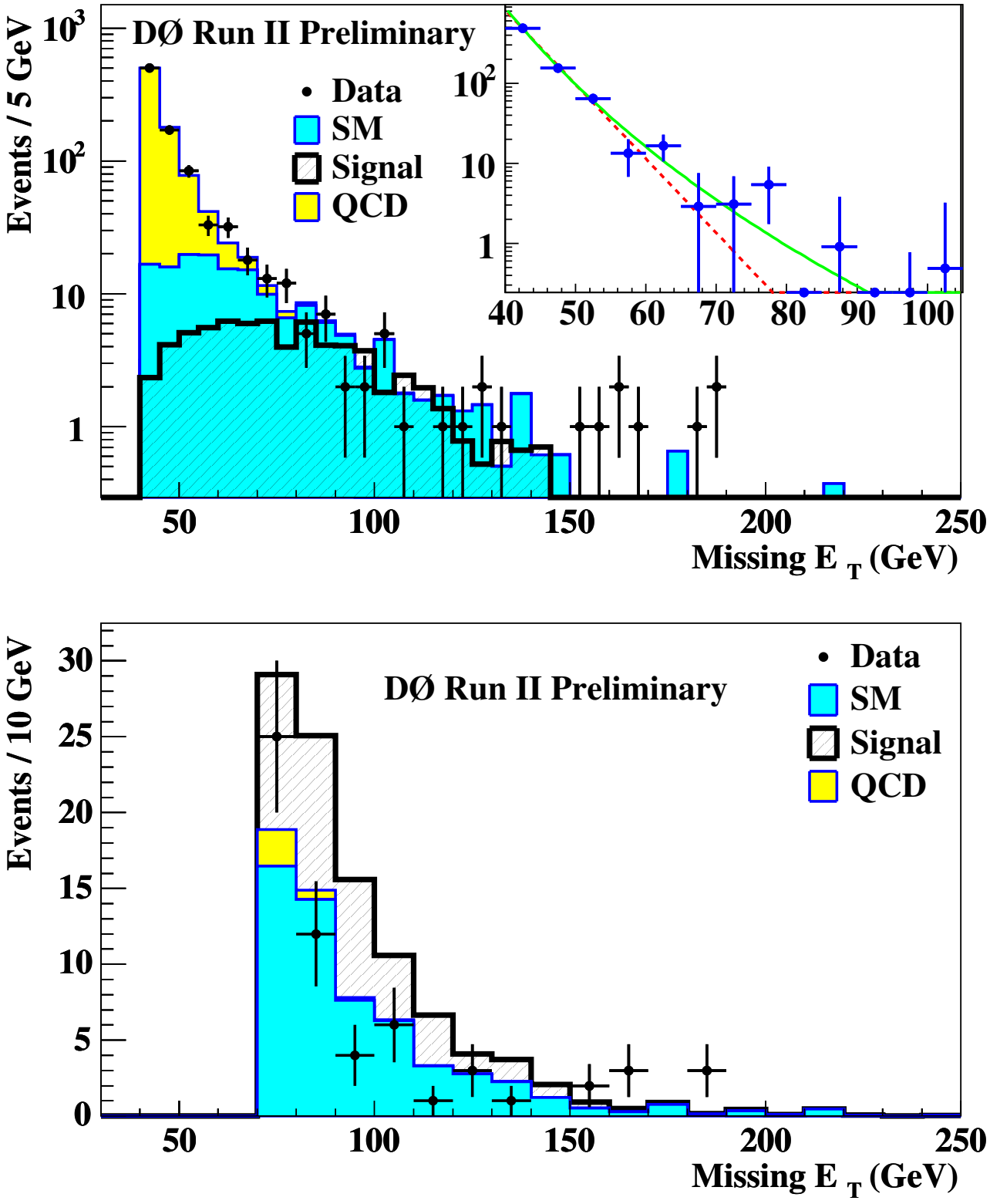

FIG. 2: Distributions of the missing transverse energy for data (points with error bars), for SM backgrounds (heavy-shaded histograms), for the instrumental background (labeled "QCD", light-shaded histograms), and for a signal with $m_{\tilde{t}} = 130$ GeV and $m_{\tilde{\chi}_1^0} = 50$ GeV. In the top frame, the $\not\!\!E_T$ distribution is marginal, the signal is displayed as a hatched histogram, and the insert shows how the instrumental background is estimated from power-law (full curve) and exponential (dashed curve) fits. The $\not\!\!E_T$ distribution in the bottom frame is after all cuts, with the same shading code but with the signal contribution now displayed on top of all backgrounds.

region. The statistical uncertainty of the signal simulation is 5%. Finally, the uncertainty on the signal efficiency due to the PDF choice was determined to be $^{+6}_{-4}$%, using the forty-eigenvector basis CTEQ6.1M PDF set [11].

C. Limits

No significant excess of data was observed for any of the stop and $\tilde{\chi}_1^0$ mass combinations considered. Limits on the stop pair production cross section have therefore been derived, in the modified frequentist CL_s approach [22]. They were compared with theoretical NLO cross sections predicted by PROSPINO with the CTEQ6.1M PDF's. The nominal cross section was obtained for $\mu_{rf} = m_{\tilde{t}}$. Theoretical uncertainties on the stop pair production cross section arise from the choices of PDF's and of renormalization and factorization scale. The variations observed with the forty-eigenvector basis CTEQ6.1M PDF set, as well as the changes induced when μ_{rf} is modified by a factor of two up or down, reflect in a typically $\pm 20\%$ change in the theoretical cross section when combined quadratically. The exclusion contour in the ($m_{\tilde{t}}$,$m_{\tilde{\chi}_1^0}$) plane is shown as a thick curve in Fig. 3 for the nominal production cross section. The corresponding expected exclusion contour is shown as a dotted curve. The effect of the PDF and scale uncertainties is shown as a yellow band.

This analysis extends the stop and $\tilde{\chi}_1^0$ mass domain excluded by previous experiments [12–14]. For the nominal stop-pair production cross section, the largest stop mass excluded is 137 GeV, obtained for $m_{\tilde{\chi}_1^0} = m_{\tilde{t}} - m_b - m_W = 52$ GeV. Taking into account the theoretical uncertainty on the production cross section, the largest stop mass limit is 131 GeV, obtained for $m_{\tilde{\chi}_1^0} = 46$ GeV. These results were derived under the assumption that the stop decays into a c quark and the lightest neutralino.

Acknowledgments

We thank the staffs at Fermilab and collaborating institutions, and acknowledge support from the DOE and NSF (USA); CEA and CNRS/IN2P3 (France); FASI, Rosatom and RFBR (Russia); CAPES, CNPq, FAPERJ, FAPESP and FUNDUNESP (Brazil); DAE and DST (India); Colciencias (Colombia); CONACyT (Mexico); KRF and KOSEF (Korea); CONICET and UBACyT (Argentina); FOM (The Netherlands); PPARC (United Kingdom); MSMT (Czech Republic); CRC Program, CFI, NSERC and WestGrid Project (Canada); BMBF and DFG (Germany); SFI (Ireland); The Swedish Research Council (Sweden); Research Corporation; Alexander von Humboldt Foundation; and the Marie Curie Program.

[1] H.E. Haber and G.L. Kane, Phys. Rep. **117**, 75 (1985).
[2] H.P. Nilles, Phys. Rep. **110**, 1 (1984).
[3] See for instance V. Barger, M.S. Berger and P. Ohmann, Phys. Rev. D **49**, 4908 (1994).
[4] J. Ellis and S. Rudaz, Phys. Lett. B **128**, 248 (1983).
[5] M. Quiros, Nucl. Phys. Proc. Suppl. **101**, 401 (2001), and references therein.
[6] P. Fayet, Phys. Lett. B **69**, 489 (1977).
[7] J. Ellis *et al.*, Nucl. Phys. B **238**, 453 (1984).
[8] K.I. Hikasa and M. Kobayashi, Phys. Rev. D **36**, 724 (1987).
[9] C. Boehm, A. Djouadi and Y. Mambrini, Phys. Rev. D **61**, 095006 (2000).
[10] W. Beenakker *et al.*, Nucl. Phys. B **515**, 3 (1998).
[11] J. Pumplin *et al.*, J. High Energy Phys. **0207**, 012 (2002); D. Stump *et al.*, *ibid.*, **0310**, 046 (2003.
[12] LEPSUSYWG, ALEPH, DELPHI, L3 and OPAL Collaborations, note LEPSUSYWG/04-02.1 (http://lepsusy.web.cern.ch/lepsusy/Welcome.html).
[13] T. Affolder *et al.* (CDF Collaboration), Phys. Rev. Lett. **84**, 5704 (2000).
[14] V.M. Abazov *et al.* (D0 Collaboration), Phys. Rev. Lett. **93**, 011801 (2004).
[15] D0 Collaboration, *"Search for Scalar Leptoquarks in the Acoplanar Jet Topology with the D0 Detector"*, D0 Note 5040-CONF.
[16] V. Abazov *et al.* (D0 Collaboration), *"The Upgraded D0 Detector"*, to appear in Nucl. Instrum. Methods in Phys. Res. A.
[17] G.C. Blazey *et al.*, in *Proceedings of the Workhop: "QCD and Weak Boson Physics in Run II,"* edited by U. Baur, R.K. Ellis, and D. Zeppenfeld (Fermilab, Batavia, IL, 2000), p. 47; see Sec. 3.5 for details.
[18] M.L. Mangano *et al.*, J. High Energy Phys. **0307**, 001 (2003).
[19] T. Sjöstrand *et al.*, Comput. Phys. Commun. **135**, 238 (2001).
[20] H.L. Lai *et al.* Eur. Phys. J. C **12**, 375 (2000).

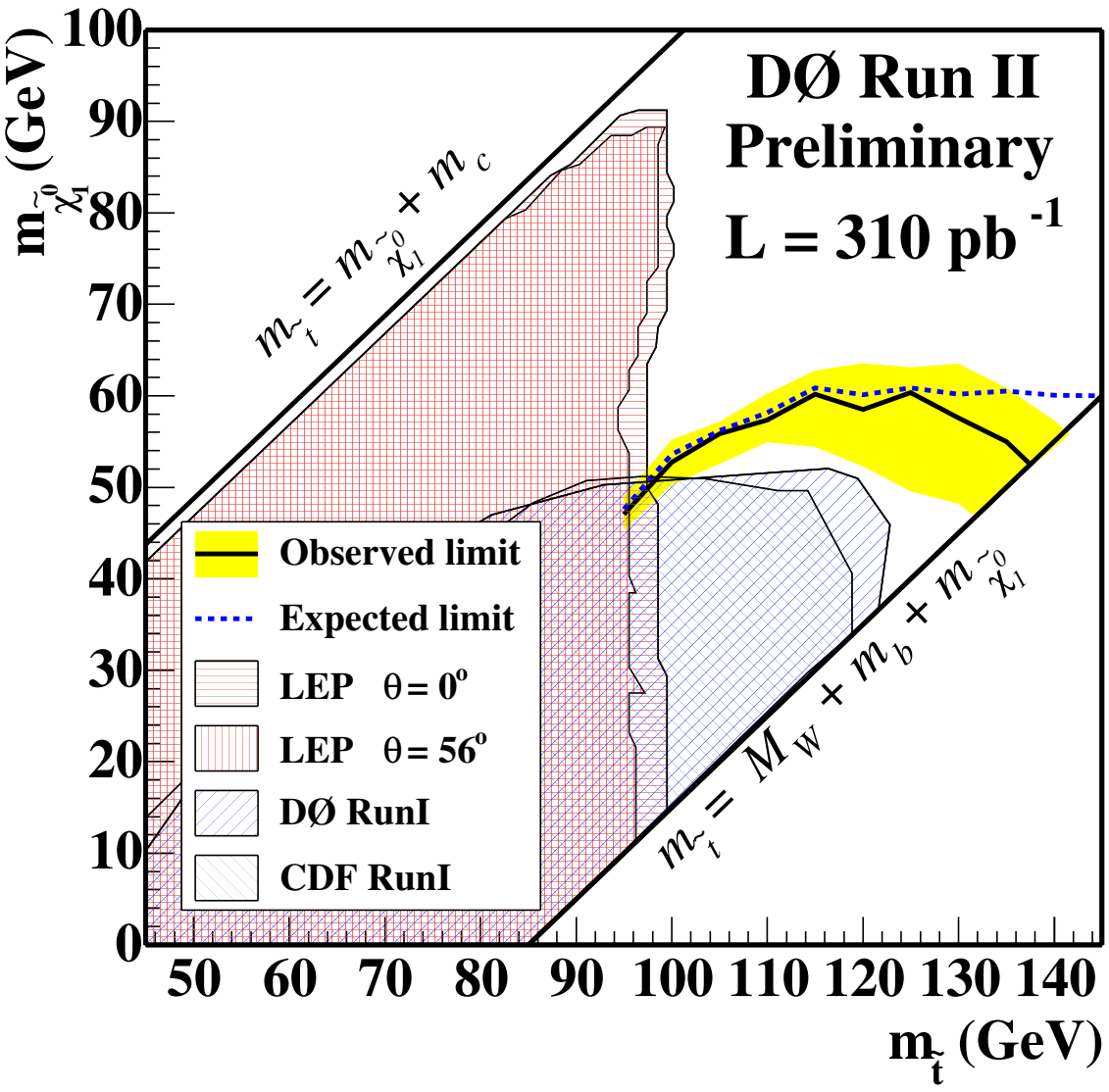

FIG. 3: Domain in the $(m_{\tilde{t}}, m_{\tilde{\chi}_1^0})$ plane excluded by the present search (thick full curve), under the assumption that the stop decays into $c\tilde{\chi}_1^0$ and for the nominal pair production cross section. The expected exclusion contour is shown as a dotted curve. The effect of increasing or decreasing the production cross section by its uncertainty due to the PDF and μ_{rf} choices is indicated for the observed exclusion contour by the yellow band. The results from previous searches for stop pair production in the $\tilde{t} \to c\tilde{\chi}_1^0$ decay channel are also indicated [12–14].

[21] J. Campbell and R.K. Ellis, Phys. Rev. D **60**, 113006 (1999).
[22] T. Junk, Nucl. Instrum. Methods A **434**, 435 (1999);
A. Read, in *"First Workshop on Confidence Limits"*, CERN Report No. CERN-2000-005, 2000.